

Contents

1	Introduction	2
2	Theory	4
2.1	Theoretical view on characteristic X-rays	4
2.1.1	Formation of characteristic X-rays	4
2.1.2	Naming convention	5
2.1.3	Energy and intensity	6
2.2	Empirical view on characteristic X-rays	7
2.2.1	From lines to peaks	11
2.2.2	Intensity	11
2.2.3	K-factors and k-ratios	13
2.2.4	Detection system	13
2.2.5	Sample thickness	13
2.2.6	Bremsstrahlung - the background radiation	13
2.3	Calibration of the spectrum	13
2.4	SEM	13
3	Method / experimental design	14
3.1	Introduction	14
3.2	Materials	14
3.3	The microscope and the detector	14
3.4	Analysis in AZtec and data extraction	15
3.5	Analysis in HyperSpy	16
3.6	Data treatment	16
3.6.1	Normalization	16
3.6.2	Gaussian fitting and peak finding	17

Chapter I

Introduction

The main goal of this project is to improve EDS analysis. There are multiple ways to improve EDS analysis, which can be qualitative, quantitative, or both. One way is to make the analysis more transparent, which would make it easier to understand and use. A second option is to improve the input parameters of the analysis by control checking the instrument with a known sample. A third way is to make the quantitative analysis more accurate, which would improve EDS analysis. In this project, the main focus have been trying to improve the transparency of the analysis. Thus, the problem statement was formulated as:

Main problem statement. How do different spectroscopy data processing influence the qualitative analysis, and how do they affect the quantitative Cliff-Lorimer analysis in HyperSpy?

Most of the time used in this project was spent on trying to understand some of the methods of data processing in EDS analysis. The different methods were applied on the same data sets to see how they influence the qualitative analysis. Towards the end the different methods were applied on the data before the Cliff-Lorimer quantification in HyperSpy to see how they influence the quantitative analysis. Solving the main problem statement with an open-source Jupyter Notebook would increase the transparency of the analysis and allow users to both adjust their analysis and understand better the analysis. The main problem statement was broken down into five sub-problems. The sub-problems and a short description follow below.

Sub-problem 1. How accurate is the out-of-the-box quantification in AZtec and HyperSpy?

Sub-problem 2. What are done with the data at the different steps in the analysis when using HyperSpy?

Sub-problem 3. How are the peaks and the background be modelled?

Sub-problem 4. How is the spectrum calibrated, and is AZtec different from HyperSpy?

Sub-problem 5. When does the analysis fail, both in AZtec and HyperSpy?

(Question for Ton: Should I have a short paragraph here about the status of EDS analysis today?)

Paragraph about why EDS in AZtec is for dummies.

(Brynjar: Paragraph about Dispersion, offset, energy resolution?)

(Brynjar: Paragraph about Other parameters of EDS analysis?)

(Brynjar: Paragraph about Improving quantitative EDS analysis?)

This remainder of this report is built up around the main problem statement and the sub-problems. The theory chapter contains the physics of X-rays and empirical adjustments in the analysis, a section on data processing, and a section about the hardware in an EDS setup. The method chapter explains how the data was collected, while the arguments for and against the different methods are presented in the discussion chapter. The result chapter contains qualitative and quantitative results. The qualitative results are presented as figures of spectra showing the elements in the sample, and also how well different calibrations fit with the theoretical values. The quantitative results are presented as tables with compositional results with different methods and adjustments. The different methods are using AZtec and two approaches in HyperSpy. The different adjustments are results with different calibrations, different background models, **(Brynjar: "and different peak models"?)** The discussion chapter follow the structure of the sub-problems, and discuss both the methods and the results of the analysis consecutively. The conclusion chapter summarizes the report with an answer to the main problem statement, and provides ideas for further work. The appendix contains the code used in the analysis, which is also available on GitHub **(Brynjar: [Link to GitHub](#))**.

Chapter 2

Theory

Energy dispersive X-ray spectroscopy (EDS) is a technique for analyzing the elemental composition of a sample with a spatial resolution, used in SEM and TEM. The technique is based on excitation of core shell electrons, which are bound to the atom with different strengths in different elements, and thus the electron relaxation results in very specific photon energies. EDS can be used to determine both the qualitative and quantitative composition of a sample. This chapter will cover the theoretical formation of characteristic X-rays, the empirical adjustments done due to creation and detection issues, explain quantitative calculations, cover the parameters of a quality control program, and briefly explain the basics of a SEM.

2.1 Theoretical view on characteristic X-rays

This section is primarily based on Hollas [3, Ch. 8.2] and Goldstein [2, Ch. 4.2]. It covers the theoretical physics behind creation of characteristic X-rays.

2.1.1 Formation of characteristic X-rays

The formation of characteristic X-rays is an inelastic quantum mechanical scattering process in two steps. In the following four equations the subscripts are referring to specific electrons in order to distinguish between them, which is also used in FIGURE XX (Brynjar: make this figure). In the first step described in Equation (2.1) electron e_1^- from the incident electron beam eject electron e_2^- from the core orbital of atom A [3, Eq. (8.12)].

$$e_{1\text{incident}}^- + A \rightarrow e_{1\text{outgoing}}^- + A^+ + e_{2\text{ejected}}^- \quad (2.1)$$

The incident electron from the beam loose energy to both breaking the binding energy of the core orbital and to the

kinetic energy of the ejected electron. The energy is given by Equation (2.2). The user can control the incident electron energy $E_{1\text{incident}}$ by the acceleration voltage V_{acc} of the electron gun (and the current I_{beam} of the electron beam). The energy of the characteristic X-ray is dependent on the binding energy of the core orbital, $E_{2\text{-core shell, binding}}$. In EDS $E_{1\text{outgoing}}$ and $E_{2\text{kinetic}}$ serve no purpose [2, Eq. (4.1)].

$$E_{1\text{incident}} = E_{1\text{outgoing}} + E_{2\text{core shell, binding}} + E_{2\text{kinetic}} \quad (2.2)$$

In the second step electron e_3^- from a higher energy orbital relaxes to the hole in the core orbital of atom A, and the difference in energy is emitted as a photon with a specific energy $h\nu$ called the characteristic X-ray [3, Eq. (8.12)].

$$e_{3\text{outer shell}}^- \rightarrow e_{3\text{inner shell}}^- + h\nu_{\text{X-ray}} \quad (2.3)$$

The energy of the characteristic X-ray is the difference in energy between the ionized orbital and the orbital filling the hole, shown in Equation (2.4). The equation specifies the energy of the X-ray as $h\nu$, but Section 2.2 explains why users of EDS just use the energy directly, usually measured in eV or keV [2, Eq. (4.2b)].

$$h\nu_{\text{X-ray}} = E_{2\text{core shell, binding}} - E_{3\text{outer shell, binding}} \quad (2.4)$$

In the second step in Equation (2.3) it is also a probability that the relaxation energy is used to eject and give kinetic energy to another electron from a higher energy orbital. This process results in two ejected electrons, both the ionized electron from the core orbital and a second ejected electron from a higher energy orbital. The second ejected electron is called an Auger electron. Auger electrons are used for surface studies, because they can penetrate around 2 nm solid material and thus does not escape from inside the sample. The X-rays are emitted in all directions and penetrate typically 4000 nm, and are the signal in EDS. The ratio between the characteristic X-ray photons and Auger electrons are known as the fluorescent (quantum) yield, ω .

$$\omega = \frac{\text{X-ray photons}}{\text{Auger electrons}} \quad (2.5)$$

The fluorescent yield is heavily dependent on the experimental setup and can be approximated, which is covered as one of the empirical factors in Section 2.2.

2.1.2 Naming convention

The transition lines are grouped and named semi-systematic, based on the orbital the vacancy is in, and the orbital the electron is relaxed from. The naming convention is semi-systematic because it is the original empirical system published in Nature by the Swedish physicist Siegbahn in 1916 [5], when they did not have the knowledge we have today. The

International Union of Pure and Applied Chemistry made a more systematic naming convention for X-ray lines which is supposed to be the official one [2, Ch. 4.2.4]. However, the Siegbahn notation is used in the X-ray booklet, in HyperSpy, and by the TEM group at NTNU, and thus is used in this thesis.

The X-rays are first named by which shell in the Bohr model the vacancy is in, i.e. the principal quantum number n of the vacancy orbital. Relaxations to the innermost shell $n = 1$ is named K-transitions, relaxations to $n = 2$ is L-transitions, relaxations to $n = 3$ is M-transitions.

The X-rays are further grouped with Greek letters in families. Orbitals close in energy are usually in the same group, which means that electrons in the same shell usually are in the same family. This naming is non-systematic, but tends to follow a pattern where the transitions labeled α are the lower energy transitions corresponding to the $n + 1$ orbitals, and the transitions labeled β are the higher energy transitions corresponding to the $n + 2$ orbitals. For example, $L \rightarrow K$ are α -transitions.

In addition, the lines in an X-ray group are labeled with subscript numbers which generally start with the highest intensity. This is a splitting of the lines due to different energy levels of the orbitals in the same shell. The different energy levels are due to the spin-orbit coupling, which is the interaction between the electron spin and the orbital angular momentum. The spin-orbit coupling increase with increased Z , which separates the lines more and more. The splitting of the α family to α_1 and α_2 are usually first resolvable in EDS for elements heavier than tin with $Z = 50$ [3, Ch. 8.2.2.3].

Putting these three naming conventions together, we name the transition $L_3 \rightarrow K_1$ as $K\alpha_1$, and $L_2 \rightarrow K_1$ as $K\alpha_2$, with more examples in Figure 2.1. The transition $L_1 \rightarrow K_1$ has $\Delta l = 0$ and is thus forbidden by the selection rules, see Equation (2.6). In gallium the $K\alpha_1 = 9251.74$ eV and $K\alpha_2 = 9224.82$ eV [7] are coupled, but as shown in Figure 2.5 this energy difference of $\Delta E = 26.92$ eV is too low to be resolved in EDS.

2.1.3 Energy and intensity

The energy of the characteristic X-ray depends on which orbital the vacancy is in, which orbital the electron is relaxed from, and the amount of protons in the core of atom A. Higher Z means higher energy of the characteristic X-ray line, because the energy difference between the relaxation orbital and the ionized orbital is larger. Atoms with higher Z have more possible transitions, because they have more electrons and orbitals.

The selection rules, which govern the allowed transitions for the formation of characteristic X-rays, are based on the Pauli exclusion principle and the spin-orbit coupling. See Figure 2.2 for illustration of the quantum number n and l which are relevant for the selection rules. Quantum number j is the total angular momentum, which is the sum of the orbital angular momentum l and the spin angular momentum s . The selection rules in Equation (2.6) is for the electron which relaxes to the vacancy in the core orbital of atom A [3, Sec. 8.2.2.2].

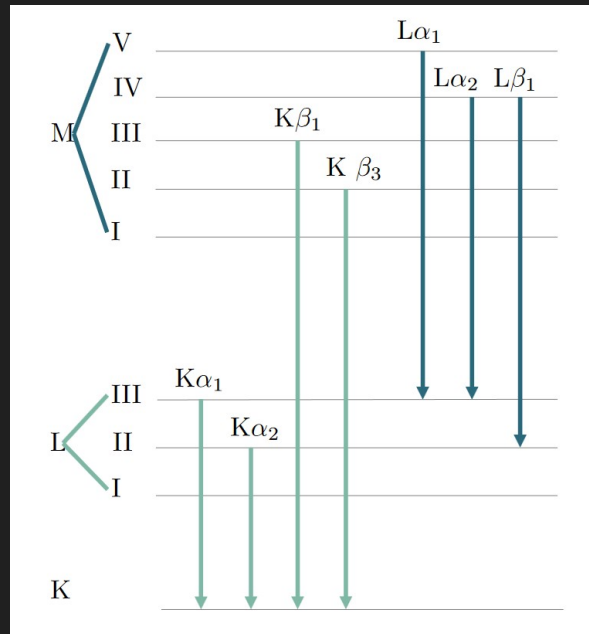


Figure 2.1: Direct copy of Maris Figure 2.9. I will make my own.

$$\Delta n \geq 1; \quad \Delta l = \pm 1; \quad \Delta j = 0, \pm 1 \quad (2.6)$$

Even though heavy atoms like gold have more than 30 possible transitions, only a few are detectable in EDS. Lines which are undetectable have low abundance, are too close to other lines, or are forbidden by the selection rules [2, Ch. 4.2.3]. Lines which are detectable have an intensity dependent on the amount of the element in the sample, because a higher amount gives more counts in the detector. The counts in EDS the number of X-ray photons detected in a specific energy range. The energy range is typically around 10 eV. In theory, the ratio of the atomic concentration between two elements are proportional to the ratio of the corresponding lines from the elements. However, there are many factors which affect the intensity of the lines, which are covered in Section 2.2.

2.2 Empirical view on characteristic X-rays

On top of the theoretical physics there are many experimental processes affecting both the creation and the detection of characteristic X-rays. The scientific community uses an empirically influenced approach in EDS analysis. This approach includes empirical equations to deal with the imperfect beam, scattering in the chamber, secondary scattering (?), imperfect detectors, ...

(Question for Ton: What do I do with the thin film assumptions? How do I mention it?)

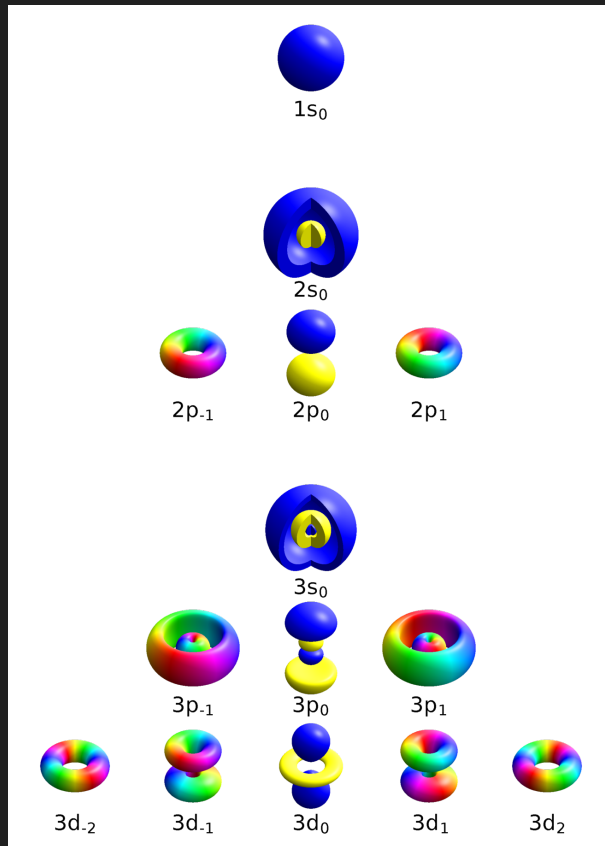


Figure 2.2: The quantum numbers n , l , and m in a hydrogen-like atom. The principal quantum number is shown as the block with values $n = 1, 2, 3$. The Azimuthal quantum number is the rows as $l = s, p, d$. The magnetic quantum number is the columns as $m = -2, -1, 0, 1, 2$. The spin quantum number, s , is not geometrically dependent and thus not shown. The total angular momentum quantum, l number is the sum of l and s . The figure is copied from the article "Quantum number" on Wikipedia, made by Geek3 - Own work, Created with hydrogen 1.1, CC BY-SA 4.0, <https://commons.wikimedia.org/w/index.php?curid=67681892>.

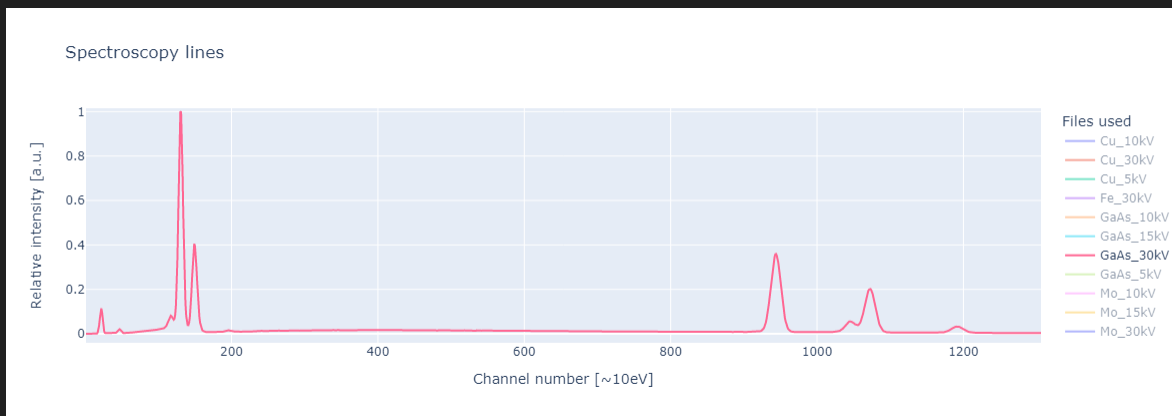


Figure 2.3: The whole GaAs spectrum. The next two figures zoom in on different parts of this plot. Data from the SEM Apreo at NTNU NanoLab, 30 kV.

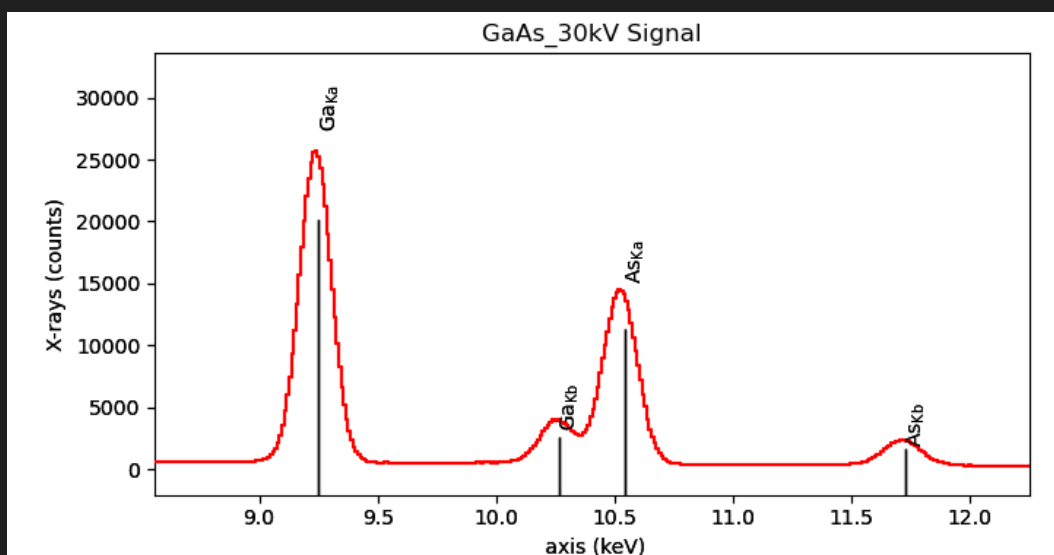


Figure 2.4: Plot produced by HyperSpy of the X-ray lines in GaAs from 8 to 12.5 keV. The theoretical lines are marked with black lines, but in reality the lines become peaks with Gaussian shapes. The height of the black lines are empirically estimated and are available in HyperSpy. Notice also how the center of the peak and the black line are slightly right shifted, which can be solved by calibrating the energy scale, see Section 2.3. Data from the SEM Apreo at NTNU NanoLab, 30kV.

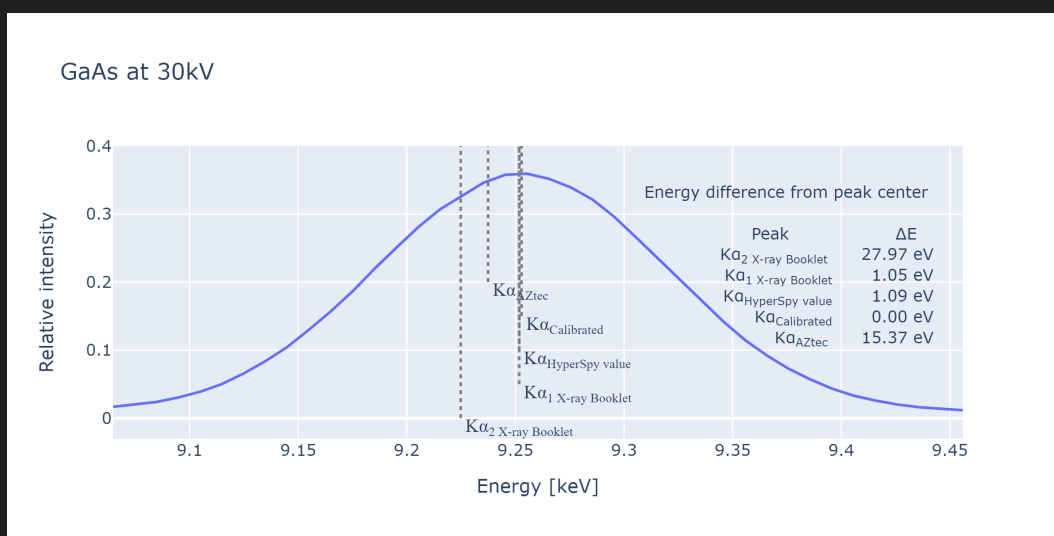


Figure 2.5: The theoretical lines $K\alpha_1 = 9.25174$ and $K\alpha_2 = 9.22482$ from the X-ray booklet with $K\alpha = 9.251$ from HyperSpy and the fitted peak $K\alpha$. The spectrum is calibrated to Ga $L\alpha$ and As $K\alpha$, where the energy of the peaks is taken from HyperSpy. HyperSpy gives Ga $K\alpha$ almost directly on top of the theoretical $K\alpha_1$. This figure show that the lines which are separated with small energy differences are so close that they make one single peak in the EDS spectrum. Data from the SEM Apreo at NTNU NanoLab, 30kV. **(Question for Ton: This is more results than theory I would say. But I do remember you saying something about having this in the theory section.)**

Table 2.1: Ga lines from HyperSpy cite ?? and X-ray booklet [7]. ** HyperSpy operates with a single line for each K and L shell, but the X-ray booklet lists two lines for each shell. * HyperSpy lists Ln , Ll and Lb_3 as separate lines, but I am not sure what they correspond to in the X-ray booklet. TODO: Figure out this, eventually just dropping the additional lines.

	X-ray booklet	HyperSpy	HyperSpy
	Energy [keV]	Energy [keV]	Weight
$K\alpha_1$	9.25174	9.2517	1.0
$K\alpha_2^{**}$	9.22482		
$K\beta_1$	10.2642	10.2642	0.1287
$L\alpha_1$	1.09792	1.098	1.0
$L\alpha_2^{**}$	1.09792		
$L\beta_1$	1.1248	1.1249	0.16704
Ln^*		0.9843	0.02509
Ll^*		0.0544	0.9573
Lb_3^*		0.0461	1.1948

2.2.1 From lines to peaks

A striking difference between the theoretical and the empirical view is that the lines are not lines, but peaks with a varying width. This is illustrated both in Figure 2.4 and in Figure 2.5, where we see that the two $K\alpha$ lines of Ga is merged into one broad peak. The peaks in the EDS spectrums have a Gaussian shape, which is a result of the broadening of the lines. The broadening of the lines is due to ... **(Question for Ton: What is the cause of the broadening? And why is it Gaussian?)**. Figure 2.3 shows that lower energy lines are narrower than higher energy lines. This increase in broadening with higher energy is due to ... **(Question for Ton: What is the cause of the broadening with higher E again?)**

(Brynjar: Write more here.) A Gaussian peak is a curve defined by the following equation:

$$g(x) = \frac{1}{\sigma\sqrt{2\pi}} \exp\left(-\frac{(x - \mu)^2}{2\sigma^2}\right) \quad (2.7)$$

In the equation μ is the center of the peak, σ is the standard deviation, and x is the energy. When doing peak fitting, the first term is treated as the amplitude and is a parameter which is fitted, i.e. $1/\sigma\sqrt{2\pi}$ is swapped with a parameter A . μ and σ are also fitted parameters, where μ is the center of the peak and σ is the width of the peak. x is the energy, i.e. the x-axis in the EDS spectrum.

The width of the peak is a measure of the broadening of the line, and is usually given as the FWHM in EDS analysis. The FWHM is connected to the standard deviation of the Gaussian distribution, which is given by Equation (2.7). The FWHM can be calculated from the standard deviation, σ , with:

$$\text{FWHM} = \sigma 2\sqrt{2 \ln(2)} \quad (2.8)$$

2.2.2 Intensity

The intensity, or weight, of a line is dependent on multiple empirical and physical factors. This subsection will briefly cover fluorescent yield, critical ionization energy, and empirical weights in HyperSpy. In practice, the weight of the lines are included as a part of the k-factors or k-ratios, which are presented in Section 2.2.3. Only the strongest lines are listed in the X-ray booklet, where the theoretical values of the characteristic X-ray lines are listed. The list include: $K\alpha_1$, $K\alpha_2$, $K\beta_2$, $L\alpha_1$, $L\alpha_2$, $L\beta_1$, $L\beta_2$, $L\gamma_1$, $M\alpha_1$ [7].

(Brynjar: This info about fluorescent yield is interesting, but will I actually use it?) The fluorescent yield ω is non-linearly dependent on Z . Figure (4.3) in Goldstein [2] **(Question for Ton: Reproduce the figure? Would take like 2h to use the Crawford data properly I guess)** shows the fluorescent yield for the first 90 elements (which is based on Crawford 2011). For K- and L-shell fluorescent yield, ω is strictly increasing. For M-shell fluorescent yield, ω is strictly increasing till around $Z = 80$, and then it starts to decrease. The figure also show that for the same element

$\omega_K > \omega_L > \omega_M$ (Brynjar: But L-peaks are higher in the spectra. Explain this in the discussion?). When dealing with thin samples, the fluorescent yield can be approximated by an empirical formula based on tin. The formula is given in Equation (2.9), where $a = 10^6$ for K-shell. (Brynjar: What is it for L and M? Also, is it really relevant here?) The two key takeaways from this formula is that ω is dependent on Z , but kinda similar for close elements like Ga $Z = 31$ and As $Z = 33$.

(Brynjar: Find the source for this formula. Ton said it is from Williams and Carter. Is it valid for bulk? The K-shell have the same shape as Figure 4.3 in Goldstein.)

(Question for Ton: I'm not sure if I will actually use this formula, should I just remove it? And I don't get how this formula just becomes a part of the k-factor. Except from the key takeaways mention above.)

$$\omega = \frac{Z^4}{a + Z^4} \quad (2.9)$$

The critical ionization energy, E_C , is the energy the incident beam need to ionize a core electron in an atom. If the energy of the incident beam is lower than E_C , the core electron is not ionized and no peak can be detected. The critical ionization energy is dependent on the atomic number, Z , of the atom. Higher Z means higher E_C , because the core electrons are bound stronger to the nucleus. When the incident beam has an energy higher than E_C and continues to increase, the amount of ionization is not constant and not linear. The amount of ionization with varying energy above E_C is dependent on the ionization cross section and the overvoltage, which again are dependent on what shell the ionization happens in. The solution to this is empirically estimations and using k-factors where all factors like this is either cancelled out or included in the k-factor correction.

(Question for Ton: Is this good enough? If not, what do I write about the ionization cross section and overvoltage? What Mari wrote is for thin samples, I think. Why include it if I'm not going to use any equations about the ionization cross section or overvoltage? You said something about just write that intensity it is lower for low energy because of many reasons (absorption, efficiency), with the same reason that background is lower for low energy. But I kinda need to explain some reasons to use them in the discussion. Another question: in the k-factor all these other factors fall out, so EDS-people does not use these equations. Am I wrong?)

HyperSpy have an integrated list of the characteristic X-rays, with both the energy and the weight of the lines. (Brynjar: I guess the weights are empirically estimated, but I have not found any information about how they are estimated. In addition: I'm not sure if HyperSpy adjust the line height to the spectrum, or if it knows that Ga $K\alpha$ are higher than As $K\alpha$ as in Figure 2.4.) Goldstein uses different intensity weights for isolated atoms, thin foils and bulk samples [2, Ch. 4.2.6], and all are dependent on the atomic number and ionized shell. One could venture down the rabbit hole of finding the theoretical weights for different lines, but that will not be done in this

thesis. Examples of the weights from HyperSpy are given in Table 2.1. **(Question for Ton: OK?)**

2.2.3 K-factors and k-ratios

About em k-factors and k-ratios.

2.2.4 Detection system

Detector efficiency, detector resolution, dead time, angle/placement of detector, beam issues, stray: secondary excitations in the sample, Si stray, holder / chamber stray detection.

2.2.5 Sample thickness

Thin vs bulk samples.

2.2.6 Bremsstrahlung - the background radiation

Why linear and why sixth order polynomial. Which are better. **(Brynjar: I might use background removal as some results, but I'm not sure. That would be comparing the different methods, and looking at smoothing of the data before removing the background.)**

2.3 Calibration of the spectrum

E_1 and E_2 is the energy of the two characteristic X-rays, and c_1 and c_2 is the channel number of the two characteristic X-rays.

$$\text{Dispersion} = \frac{E_2 - E_1}{C_2 - C_1} \quad (2.10)$$

Get as little extrapolation as possible by selecting the longest possible distance between the two characteristic X-rays, while still using peaks with good signal-to-noise ratio. **(Brynjar: Quantify signal-to-noise ratio?)** Assume calibration on one spectrum and use it on all spectra for the same instrument.

Zero-offset in channels is:

$$\text{Zero-offset in channels} = C_1 - E_1 \cdot \text{Dispersion} \quad (2.11)$$

2.4 SEM

- how (e-beam, vacuum, ...) - hardware (scanning coils, astigmatism) - imaging (contrast, SE, BSE)

Chapter 3

Method / experimental design

3.1 Introduction

The data needed in this project was SEM EDS spectra. The spectra were acquired on a SEM APREO at NTNU NanoLab. The spectra were from a sample containing different sections with different elements to get different spectra to work with. Thanks to Mari Skomedal [6] and Martin Lundebj [4] who made manuals for easily extracting data from AZtec. The relevant material for data extraction is available on the GitHub repository for this project (ref). The data is also available on the GitHub repository for this project, under the folder `data/2022-09-06_EDS-Apreo`. This method chapter describes the material used, the microscope and detector, the analysis in AZtec and HyperSpy, and the post data treatment.

3.2 Materials

EDS data was collected on one sample with different sections containing different materials. A half 2" Si wafer was mounted with Cu tape on an Al FIB stub. On the Si wafer a smaller piece of a GaAs wafer was mounted with Cu tape. A Mo disk was mounted to the Si wafer with Ag paint. In the middle of the Mo disk there was a hole where a TEM grid was mounted. The TEM grid had GaAs nanowires on it, and the grid was made of Mo with C film. Growth of the GaAs nanowires is described in [6, Ch. 3]. A schematic of the sample is shown in Figure 3.1.

3.3 The microscope and the detector

The data in this project was collected with the SEM Apreo from FEI with an Oxford EDX detector at NTNU NanoLab. The detector is an EDX Oxford Xmax 80 mm² Solid angle detector, with reported energy resolution of 127 eV (Cite:

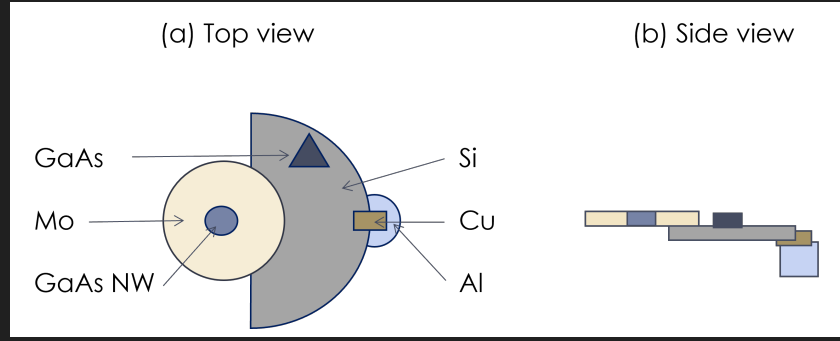


Figure 3.1: The sample used for the EDS data collection in the SEM Apreo. (a) is top view and (b) is side view. GaAs is a piece of a GaAs wafer. Mo is a Mo disk. GaAs NW is the TEM grid of Mo with C film and GaAs nanowires. Si is the Si wafer. Cu is the Cu tape. Al is the Al FIB stub. Four spectra with different V_{acc} was collected on the GaAs, Mo, Si, and GaAs NW. Three spectra was taken on the Cu tape and one spectrum on the Al FIB stub.

ntnu.norfab.no on the instrument). The acceleration voltage, V_{acc} , can be set from 0.2 to 30 kV. The beam current, I_{beam} , has a maximum value of 400 nA. The SEM has an adjustable working distance. The SEM is equipped with a BSE and a SE detector.

The data collection was done on 5, 10, 15, and 30 kV. The beam current was 0.2, 0.4, 0.8, or 1.6 nA, depending on the dead time of the detector, trying to get the dead time around 30%. Dead time at around 30% was recommended by the supervisor of this project, Antonius T. J. von Helvoort, and is well below the problematic dead time of >60%. The dead time on the nanowire area was closer to 20%, which is what Goldstein [2, page 223] recommends. All samples were collected on 2048 channels ranging from 0 to 20 keV. Working distance was 10 mm. Processing time was set to 5 and each spectrum was collected with 2 minutes time live. Some spectra were stopped early due to high dead time and thus very long sampling. At least one SE picture was taken for each sampling area. Counts per second in and out was noted down, but not used in this project. See table 3.1 for the settings used for the different spectra.

3.4 Analysis in AZtec and data extraction

The results from AZtec was taken as described in [4, Appendix A]. Both qualitative and quantitative results were acquired. The quantitative results were acquired after selecting the elements in the sample and noted as atomic percent. The k-factors calculated theoretically by AZtec was noted down, as they are needed for the quantitative analysis in HyperSpy. (Brynjar: Uncertainties? Also get this data properly from AZtec.)

3.5 Analysis in HyperSpy

The data was analyzed in HyperSpy, both qualitative and quantitative. The qualitative analysis was done by loading the spectra and plotting with lines marking the theoretical peak center and empirical weight. The quantitative analysis was done in different ways, and just on the GaAs bulk spectra. All the quantitative analysis was done with the k-factors from AZtec. The first way was to use the area under the peaks in the raw spectra, where the background was removed linearly. The second way was to make a fitted model of the background and the peaks as Gaussian curves, and use the area under the peaks in the model. Then the x-axis spectrum was calibrated, and the two ways of quantification was used again. The different calibrations used was a model fit calibration in HyperSpy, a self-made calibration and the calibration from AZtec. (Brynjar: Uncertainties from HyperSpy?)

3.6 Data treatment

In this project the data was also analyzed with new code, which is available on the GitHub profile of the author, <https://github.com/brynjarmorka/>. The end goal of this code is to improve understanding of the process. The code is written in Python and uses Jupyter notebooks. HyperSpy 1.7.1 was used for the analysis. NumPy 1.22.4 is used for calculations, SciPy 1.9.0 for fitting and peak finding, and Plotly 5.10.0 for plotting (Question for Ton: do I reference these packages?). The repository "eds-analysis"¹ contains the code developed throughout the semester, and the repository "eds-analysis-final"² contains the final code. The final code is the code which is intended to enhance a users understanding of the analysis steps. (Brynjar: Make the "eds-analysis-final" repository public.)

3.6.1 Normalization

Since the total amount of counts in a spectrum differs with V_{acc} , I_{beam} , DT, etc., the spectra had to be normalized to be able to compare them. Initially the spectra were normalized to the highest peak in each spectrum, $Intensity_{relative\ to\ max} = Counts_{raw}/Counts_{max}$. Later other normalization methods were explored, but since the quantitative analysis is based on the area under the peaks, it does not matter how the spectra are normalized. However, for the SciPy function `curve_fit` to work, the spectra had to be normalized and the raw channel numbers used as x-axis. This was probably due to the fact that the function `curve_fit` is not designed for spectra with a large dynamic range. Whatever normalization method is used, the quantitative results would be the same because of the use of peak ratios. (Question for Ton: This is getting argumentative, but it is the base for the decision and not really anything with the end results. It is just to reproduce. OK?)

¹<https://github.com/brynjarmorka/eds-analysis/>

²<https://github.com/brynjarmorka/eds-analysis-final>

3.6.2 Gaussian fitting and peak finding

The fitting of a model to the spectra was done progressively more and more advanced. All the peaks was fitted as Gaussian curves, and the fitting itself was done with the SciPy function `curve_fit`. The first model fitting was just making a Gaussian at two specified peaks. The second model was fitting a Gaussian at all the peaks in the spectrum, but still with a user input of the peak positions. The third model was fitting a Gaussian at all the peaks in the spectrum, but with the peak positions found by the SciPy function `find_peaks`. The problem with these models was that one of the peaks was usually moved to compensate for the background. Thus, the forth model was made, where the background was fitted as a sixth order polynomial. The background was fitted after removing the peaks, and then the peaks were fitted on top of the background. The fifth and final model was fitting the peaks and background in one go. The background was fitted as an n-order polynomial, and different orders were tested.

3.6.3 Calibration

A third repository, "spectroscopy-channel-calibration"³, was made specifically for calibration of spectra, which was used in the course "TFY4255 - Materials Physics" at NTNU, October 2022. The model used in this calibration is the first model from 3.6.2, and thus is not as advanced as the model used in the final code. The calibration is done with a spectrum of known elements where the user inputs the energy of the peaks. The user further specifies the channel value of two peaks. The energy of the peaks are available through HyperSpy, or can be set manually from e.g. the X-ray booklet. The code makes a Gaussian fit to the two peaks, to find the true peak center. A plot of the spectrum and the fit are shown, and the user can decide if the fit is good enough. The code then calculates the dispersion, and the zero-offset. In the end the code plots the spectrum with the calibration, and the user can decide if the calibration is good enough. The same calibration principle is implemented in "eds-analysis-final", but without the plots and the user interaction. **(Brynjar: Implement the sentence above.)** The final calibration is using the fifth model with both background and peaks in one fit. However, since the calibration only needs the distance between two peaks, using the first model could be sufficient.

3.6.4 Area under the peaks

A function finding the area under the peaks was made as a simple first step in a quantitative analysis. This simple analysis was used to quantify if different calibrations gave different results. **(Brynjar: Do this.)** Implementing the Cliff-Lorimer method for quantification was not done, but could be done in the future. The author started to look at implementation of a factorless quantification method, but did not have time to dive deep enough into that in this project.

³<https://github.com/brynjarmorka/spectroscopy-channel-calibration>

Chapter 4

Results

The results are presented in this chapter. The results are presented as plots and tables, and explained in the text. First qualitative then quantitative results are presented. All the spectra taken were qualitatively analyzed. Only the GaAs bulk spectra was quantitatively analyzed. The qualitative analysis starts with the calibration of the spectra, and then the spectra from the six sampled areas are presented. The quantitative analysis starts with analysis done in AZtec, then show how the ratio of Ga to As singal is connected to the k-factors, and finally a quantitative analysis is done with the CL method in HyperSpy of the GaAs bulk spectrum.

4.1 Qualitative analysis of the spectra

This qualitative section presents first the initial plots of the spectra done in AZtec and with HyperSpy, then the different calibrations and how well they match the theoretical vaules, and finally the spectra from the studied materials. The spectra are presented as plots and the calibrations are presented in tables.

4.1.1 Initial plot

The initial plots are only showing the GaAs 30 kV spectrum, while all the spectra are plotted in [Section 4.1.3](#). These two plots use the same calibration, which is the one from AZtec.

(Brynjar: Take a screenshot of the AZtec plot of GaAs 30 kV.)

The spectrum from the GaAs bulk wafer taken on 30 kV is shown in [Figure 4.1](#). This plot was made with HyperSpy, which utilize Matplotlib for plotting. The plotting in HyperSpy can add the theoretical peak centers as vertical lines, which is done in the plot for Ga and As. The height of the line show an estimate of the weight of the peak. In the plot it is clear that the calibration is somewhat off, since the line positions does not match the center of the peaks. In the

following section, the spectrum is recalibrated with self produced code using Scipy, and plotted with Plotly to more clearly visualize the spectra details.

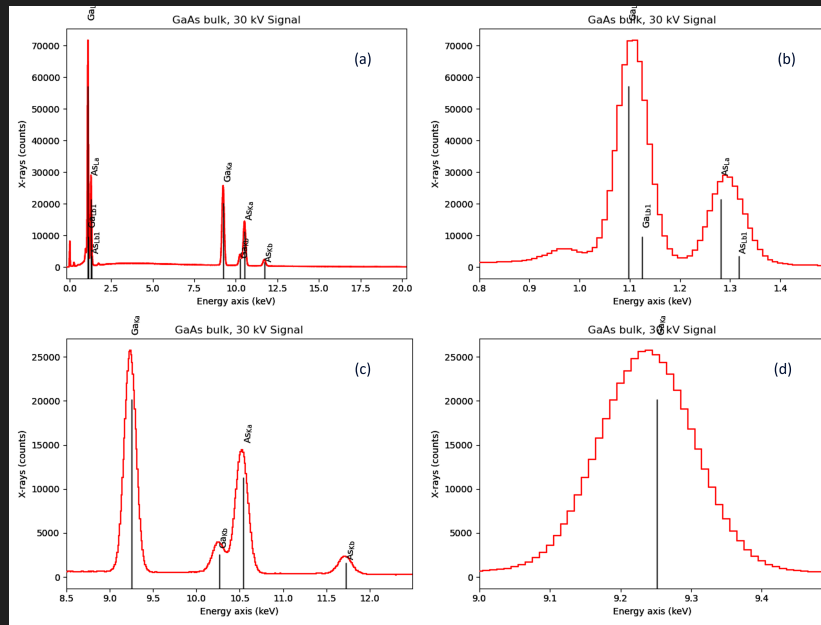


Figure 4.1: The GaAs bulk spectrum taken at 30 kV. The vertical lines are the theoretical peak centers, with weights as heights. (a) whole spectrum. (b) cropped to the L-peaks. (c) cropped to the K-peaks. (d) Ga $K\alpha$ peak. This plot has the calibration from AZtec, and it is clear that the line position is deviating from the center of the peaks. This plot was made with HyperSpy, which utilize Matplotlib.

4.1.2 Calibration

Different calibrations were explored. The initial calibration is the one from AZtec, and is the one used in the spectra in Figure 4.1. The AZtec calibration has a left shift for the L-peaks and a right shift for the K-peaks. The second type of calibration is the one given by the model fit in HyperSpy. The third type is from the self-made model fit, using the distance between two high intensity and far apart peaks to calibrate the energy scale. The third type is both calculated with the Ga $L\alpha$ and As $K\alpha$ peaks in the GaAs 30 kV spectrum, and with Mo $L\alpha$ and Mo $K\alpha$ peaks in the Mo 30 kV spectrum.

Values for the four calibrations are given in Table 4.1, i.e. the dispersion and the offset. The deviations are a some eV, and the accuracy of the different calibrations give on specific peaks are given in Table 4.2. Here accuracy is the difference between the theoretical peak position and the peak center in the spectrum, given in eV. The percentage deviation is also given. At the bottom of the table the root mean square deviation (RMSD) is given. For almost all the peaks, the deviation is greatest for the AZtec calibration. One exception is the C $K\alpha$ peak, which deviates a lot less for the AZtec calibration. The difference between the HyperSpy calibration and the self-made calibration on the GaAs is small. In

the qualitative section, the effect of the different calibrations on the spectra are explored.

4.1.3 Spectra from the studied materials

Figure 4.2 to Figure 4.8 shows the spectra for the six different areas of the sample plotted with Plotly. The plots are available as an interactive HTML plots on the GitHub repository ([Brynjar: Upload the HTML files to the GitHub repository](#)). The calibration used in these spectra is one with the lowest RMSD, which is the one from the self-made model fit on GaAs. The y-axis is normalized to the highest peak value in each spectrum, i.e. the highest peak is always 1. The spectra are cropped to show the region of interest for the different materials. Peaks which are taller than the y-axis are marked with a gray dashed line. The annotated energy on the plots is the theoretical energy of the peak, and not the fitted peak center. Some of the black annotation lines are visually offcenter on the peaks, which is due to the peak deviation previously shown in Table 4.2. The terms peak and signal is used to differentiate between well defined peaks and signals with low signal-to-noise ratio. The differentiation between peak and signal is not quantified with a threshold in this work. The annotations with an asterisk (*) are the peaks which have not theoretical value, e.g. a sum peak. First the spectra from the pure samples are presented, then the GaAs bulk wafer, and finally the GaAs NW. The order are: Al, Si, Cu, Mo, GaAs bulk, GaAs NW.

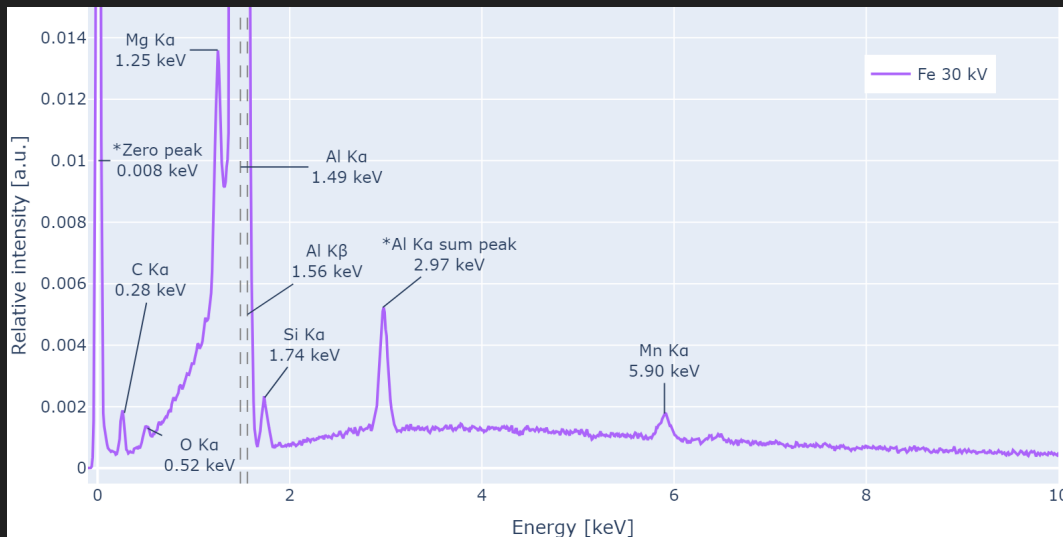


Figure 4.2: The 30 kV spectrum from the Al FIB stub. The peaks are annotated with the theoretical energy. The sum peak and zero peak are annotated with an asterisk, as they do not have a theoretical value. The dashed lines mark Al $K\alpha$ and $K\beta$, which together form one peak with relative intensity 1. (Question for Ton: Should I write SEM APREO in the figure text?)

The Al spectrum from the FIB stub is shown in Figure 4.2. As all the other spectra, this spectrum have a zero peak, a C $K\alpha$ peak at 0.260 keV and a O $K\alpha$ peak at 0.51 keV. Most of the other spectra also have a Si $K\alpha$ peak at 1.74 keV. The tallest peak with a relative intensity of 1 is the combined peak of Al $K\alpha$ and $K\beta$ at 1.49 keV. The contribution of

Table 4.1: Different calibration values. The dispersion is calculated with Equation (2.10). The offset is calculated with Equation (2.11). The own calibration was done on Ga $L\alpha$ and As $K\alpha$ from the 30 kV measurement on the GaAs wafer. The HyperSpy calibration was done by making a model and fitting it to the data on the 30 kV GaAs spectrum.

Calibration method	Dispersion, [keV/channel]	Zero offset [channels]
AZtec	0.010000	20.000
HyperSpy	0.010028	21.079
Calibration on Ga $L\alpha$ and As $K\alpha$	0.010030	21.127
Calibration on Mo $L\alpha$ and Mo $K\alpha$	0.010040	21.076

Table 4.2: Peak accuracy of the different calibration methods on 30 kV spectra: NW, Mo, Si, Al, Cu. The other acceleration voltages gave similar results. The accuracy here is the deviation from the theoretical peak to the measured peak. The percentage deviation is also given. The measured peak is the fitted center of the peak. The self-made calibration was done on two spectra: GaAs and Mo. The HyperSpy calibration was done on the GaAs spectrum. At the bottom the RMS of the deviation in the column is given.

Peak	Theoretical [keV]	AZtec [eV]	HyperSpy [eV]	Ga $L\alpha$ & As $K\alpha$ [eV]	Mo $L\alpha$ & Mo $K\alpha$ [eV]
As $L\alpha$	1.2819	12.8, 1.0%	5.6, 0.4%	5.4, 0.4%	7.2, 0.6%
As $K\alpha$	10.5436	-21.3, -0.2%	-2.7, -0.0%	-1.1, -0.0%	9.8, 0.1%
Ga $L\alpha$	1.098	11.5, 1.0%	3.8, 0.3%	3.5, 0.3%	5.1, 0.5%
Ga $K\alpha$	9.2517	-14.2, -0.2%	0.9, 0.0%	2.2, 0.0%	11.9, 0.1%
Cu $L\alpha$	0.9295	16.4, 1.8%	8.3, 0.9%	8.0, 0.9%	9.4, 1.0%
Cu $K\alpha$	8.0478	-9.2, -0.1%	2.5, 0.0%	3.7, 0.0%	12.1, 0.2%
Mo $K\alpha$	17.4793	-56.8, -0.3%	-18.8, -0.1%	-15.8, -0.1%	1.9, 0.0%
Mo $L\alpha$	2.2932	24.0, 1.0%	19.7, 0.9%	19.7, 0.9%	22.5, 1.0%
Si $K\alpha$	1.7397	2.9, 0.2%	-3.0, -0.2%	-3.2, -0.2%	-1.0, -0.1%
Al $K\alpha$	1.4865	3.0, 0.2%	-3.7, -0.2%	-3.9, -0.3%	-1.9, -0.1%
Cu $K\alpha$	8.0478	-9.3, -0.1%	2.4, 0.0%	3.5, 0.0%	11.9, 0.1%
C $K\alpha$	0.2774	-8.2, -3.0%	-18.3, -6.6%	-18.7, -6.7%	-17.9, -6.5%
RMS [eV]		14.75	4.62	4.55	9.57

Al $K\beta$ to Al $K\alpha$ is 0.013, which is small, but still changes the peak shape. There are some signal at 6.40 keV, which is where Fe $K\alpha$ would be, but here the signal-to-noise level is low. The signal at 6.40 keV is around 20% higher than the background, where the background have counts from 150-180 and the signal has 210-220 counts. The peaks at 1.25 keV and 5.9 keV indicate that there was Mg and Mn in the sample, either as impurities or as part of the alloy. The last peak in the spectrum is the Al $K\alpha$ sum peak at 2.97 keV. The background is increase rapidly and almost linearly from C $K\alpha$ to Al $K\alpha$, and drops to 10% after the Al $K\alpha$ peak. The figure also show that the Al $K\alpha$ absorbs some of the background signal right after the peak.

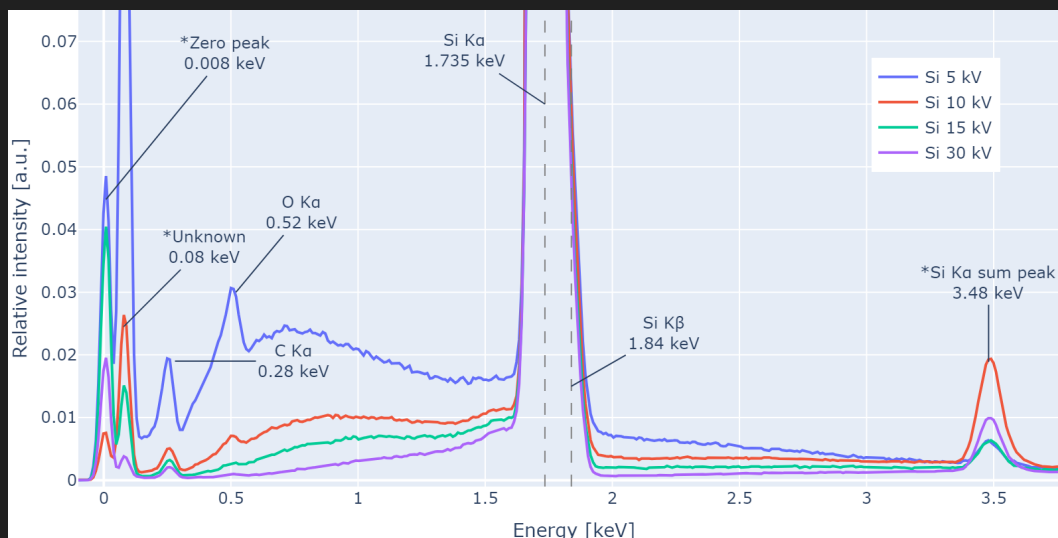


Figure 4.3: The spectra of the pure Si wafer, taken at 5 (blue), 10 (red), 15 (green), and 30 (purple) kV. **(Question for Ton: Isn't repeating the legend in the figure text a bit redundant?)** The peaks are annotated with the theoretical energy. The sum peak, unknown peak and zero peak are annotated with an asterisk, as they do not have a (known) theoretical value. The dashed lines mark Si $K\alpha$ and $K\beta$, which together form one peak with relative intensity 1.

The Si spectra from the pure Si wafer sample area is shown in Figure 4.3. As in the other spectra, this spectrum have a zero peak, a C $K\alpha$ peak at 0.260 keV and a O $K\alpha$ peak at 0.51 keV. In addition, there is an unidentified peak at 0.080 keV. The tallest peak with a relative intensity of 1 is the Si $K\alpha$ peak at 1.73 keV, which have a contribution from the $K\beta$ peak at 1.84 keV. The relative weight for Si $K\beta$ to $K\alpha$ is 0.028. As in the Al spectrum, the Si spectra have a sum peak from the tallest peak. The sum peak is at 3.48 keV, which is the sum peak of the Si $K\alpha$. In all four spectra the background drops significantly after the Si $K\alpha$ peak. The relative drop down is biggest in the 30 kV spectrum. The plot show that the background level is dependent of the acceleration voltage, at least when the spectrum is normalized to the tallest peak.

The Cu spectra from the Cu-tape is shown in Figure 4.4. These spectra have a zero peak, a C $K\alpha$, a O $K\alpha$ peak and a small Si $K\alpha$ peak. The tallest peak with a relative intensity of 1 is the C $K\alpha$ peak at 0.26 keV. The Cu $K\alpha$ and Cu $K\beta$ peaks are only visible at the 30 kV spectrum. The height of the Cu $K\alpha$ peak is 0.017, which means that the C $K\alpha$ peak is more

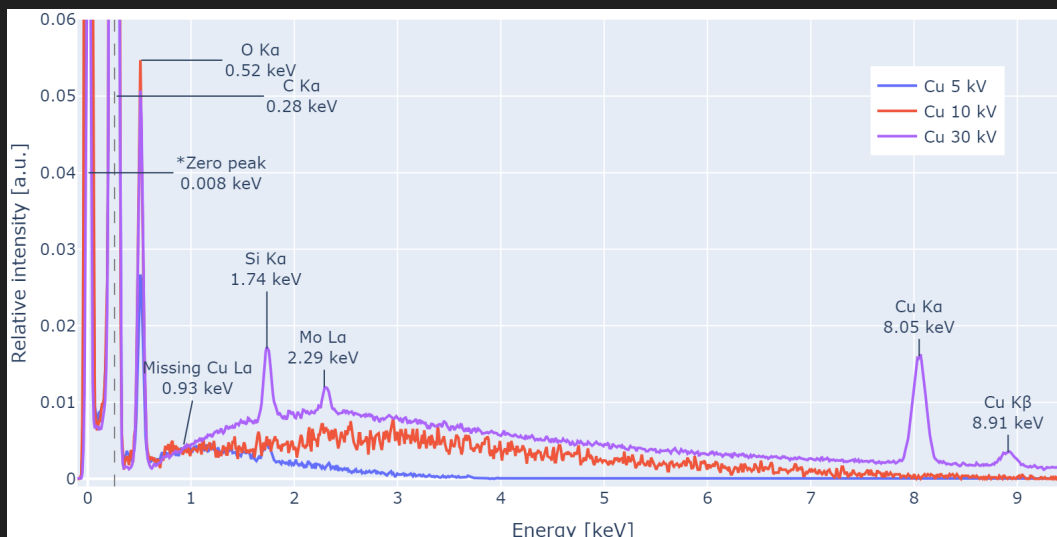


Figure 4.4: The spectra of the Cu-tape, taken at 5 (blue), 10 (red), and 30 (purple) kV. The peaks are annotated with the theoretical energy. The zero peak is annotated with an asterisk, as it does not have a theoretical value. The dashed line mark the C $K\alpha$ peak. The expected, but missing, Cu $L\alpha$ peak is marked.

than 55 times taller. None of the spectra have a Cu $L\alpha$ peak, which should have been at 0.93 keV. The 30 kV spectrum have a signal at 2.29 keV, which could be from Mo $L\alpha$, but no Mo $K\alpha$ signal is visible. In these spectra the background is highest at the 30 kV spectrum, which is the opposite as for the Si spectra. The peak heights look dependent on the acceleration voltage, but the plot hides the fact that the DT is not equal for all spectra.

The Mo spectra from the Mo disk is shown in Figure 4.5. The four spectra have a zero peak, a C $K\alpha$, a O $K\alpha$ peak. The Si $K\alpha$ give a very small signal, and is visible as the tiny peak before Mo $L\alpha$. The background of the 5 kV spectrum is very high, but that is due to its lower signal on the Mo $L\alpha$, making the 0.18 keV peak the tallest and thus scaling up the background. In other words, the 5 kV spectrum is scaled to another peak, because the Mo $L\alpha$ peak is low. The tallest peak in the 5 kV spectrum is the 0.18 keV peak, which is also visible in the other three spectra. The energy of 0.18 keV only match with the B $K\alpha$ line at 0.1833 keV. The tallest peak in the 10, 15 and 30 kV spectra is the Mo $L\alpha$ peak at 2.29 keV, which is contributed by the Mo $L\beta_1$ peak at 2.39 keV. This peak is a double peak, i.e. a peak with two overlapping Gaussian which is barely distinguishable. The HyperSpy database have the energy and weight of two other Mo peaks visible in the spectrum, which are the Mo $L\gamma_1$ and Mo $L\gamma_3$ peaks at 2.01 keV and 2.83 keV. The X-ray Booklet does not include these lines, but include some other lines which are not visible in these spectra. This difference between the listed lines in the X-ray Booklet and the lines in the HyperSpy database can be confusing and is part of the discussion in Chapter 5. Only the 30 kV spectra have a signal at the Mo $K\alpha$ and Mo $K\beta$ peaks at 17.46 and 19.62 keV. The peak at 4.6 keV is the sum peak of Mo $L\alpha$ and Mo $L\beta_1$. As in the other spectra, the background drops significantly after the tallest peak.

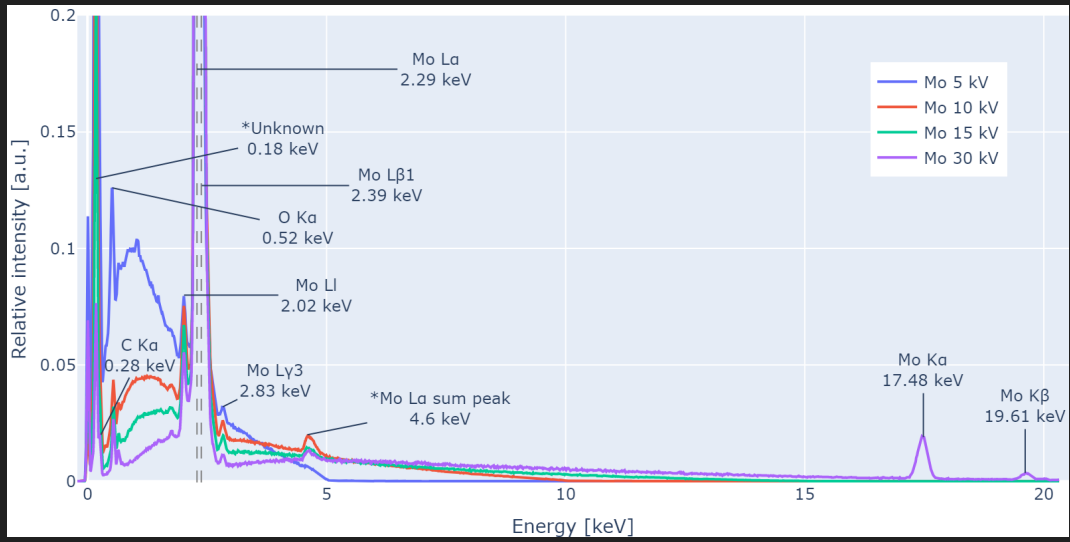


Figure 4.5: The spectra of the Mo disk, taken at 5 (blue), 10 (red), 15 (green), and 30 (purple) kV. The peaks are annotated with the theoretical energy. The sum peak, unknown peak and zero peak are annotated with an asterisk, as they do not have a (known) theoretical value. The dashed lines mark Mo $L\alpha$ and Mo $L\beta_1$, which are barely distinguishable and have a relative intensity in the 30 kV spectrum of 1 and 0.45, respectively. The background of the 5 kV spectrum is higher than the other spectra, which is due to the normalization to the tallest peak, because the tallest peak in the 5 kV spectrum is not Mo $L\alpha$, but the peak at 0.18 keV.

The GaAs spectra is shown in Figure 4.6 and Figure 4.7. The second figure is the same data with a lower y-axis and wider x-axis interval, to better visualize the background and sum peaks, and also show the K-line sum peaks. Compared to Figure 4.1, the peaks fit better with the theoretical values, which is quantified in Table 4.6. All the spectra have a zero peak, a C $K\alpha$ peak, and an O $K\alpha$ peak. The Ga $L\gamma$ peak at 0.96 keV is visible in all four spectra. The Si $K\alpha$ peak is small in all the spectra, but strongest in the 30 kV spectrum and weakest in the 5 kV spectrum. The tallest peak in all four spectra is the Ga $L\alpha$ peak at 1.1 keV. The As $L\alpha$ peak has a decreasing relative intensity from 5 to 30 kV. For the first 2 keV the background is relatively highest in the 5 kV spectrum and decreases with increasing voltage. After 2 keV this trend reverses, and the background is highest in the 30 kV spectrum. The K peaks are visible in the 15 and 30 kV spectra. The sum peaks of the L peaks are visible in the 5, 10 and 15 kV spectra, but not in the 30 kV spectrum. The sum peaks of the K peaks are only visible in the 30 kV spectrum.

The GaAs nanowire spectra are shown in Figure 4.8. This is the spectra with the most peaks, and contains signal from C, O, Ni, Cu, Ga, As, Si, Mo and Sb. One of the peaks is at 0.389 keV, which could be N $K\alpha$ peak, but it could also be other elements. The Ni signal is both from the $L\alpha$ at 0.85 keV and the $K\alpha$ at 7.49 keV. The Sb signal is from the $L\alpha$ at 3.6 keV, $L\beta_1$ at 3.8 keV, and Sb $L\beta_1$ at 4.1 keV. The Mo signal is both from the $L\alpha$ at 2.29 keV and the $K\alpha$ at 17.47 keV, but the K peak is very weak and thus not included in the plot. The Cu signal is both from the $L\alpha$ at 0.92 keV and the $K\alpha$ at 8.05 keV. The tallest peak in all four spectra is the Ga $L\alpha$ peak at 1.1 keV. In the 5 kV spectrum the C $K\alpha$ peak at

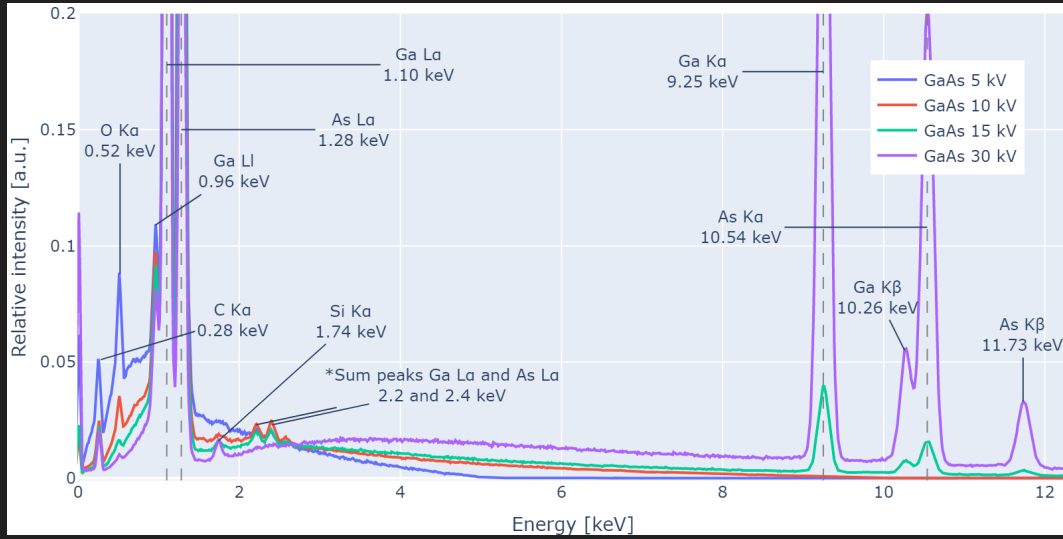


Figure 4.6: The spectra of the GaAs bulk, taken at 5 (blue), 10 (red), 15 (green), and 30 (purple) kV. This is a GaAs wafer, where the ratio of Ga to As is 1:1. The peaks are annotated with the theoretical energy. The sum peak, unknown peak and zero peak are annotated with an asterisk, as they do not have a (known) theoretical value. The dashed lines mark Ga $L\alpha$, As $L\alpha$, Ga $K\alpha$, and As $K\alpha$, with relative intensities in the 30 kV spectrum at 1, 0.41, 0.36, and 0.20, respectively.

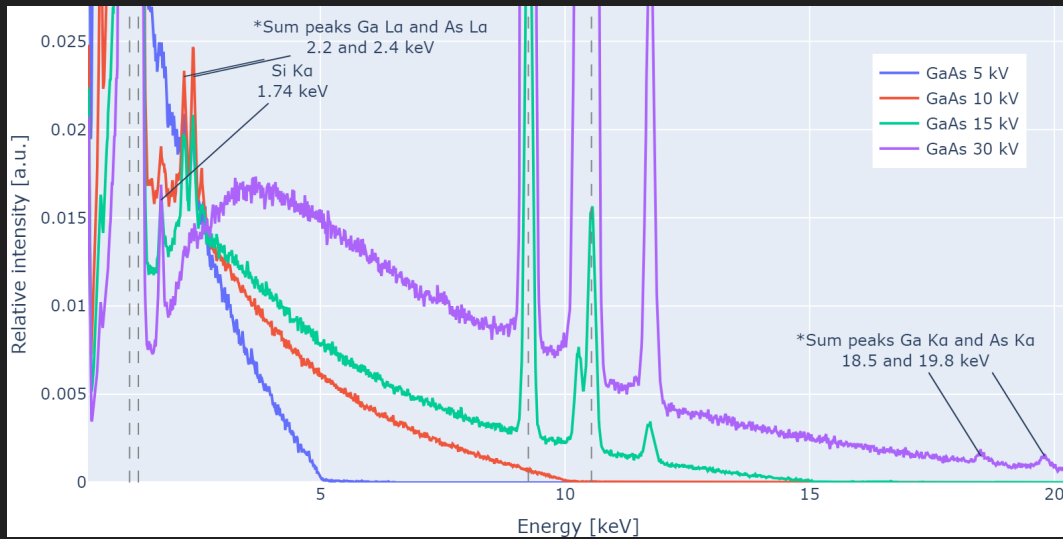


Figure 4.7: A cropped in view of the GaAs bulk spectra in Figure 4.6, but with the whole x-axis to show the K-line sum peaks. This plot is to better visualize the background and sum peaks.

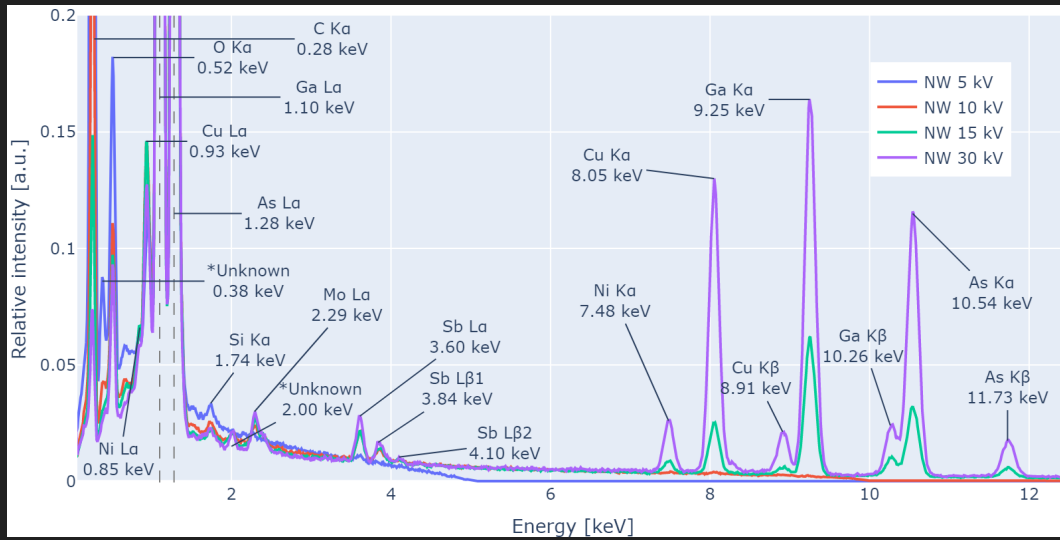


Figure 4.8: The spectra from the nanowire, taken at 5 (blue), 10 (red), 15 (green), and 30 (purple) kV. The peaks are annotated with the theoretical energy. The two unknown peaks and zero peak are annotated with an asterisk, as they do not have a known theoretical value. The dashed lines mark Ga $L\alpha$ and As $L\alpha$, with relative intensities in the 30 kV spectrum at 1 and 0.82.

0.26 keV is equally high as the Ga $L\alpha$ peak. The As and Ga signals and their ratios are very similar to the GaAs spectrum signal, but the sum peaks are not visible in the NW spectra. The Ga and As $L\alpha$ sum peaks could have been visible, but the sum peak signal coincides with the Mo $L\alpha$ peak at 2.2 keV. The 10, 15 and 30 kV signal have an unidentified peak at 2.00 keV, between Si $K\alpha$ and Mo $L\alpha$.

4.2 Quantitative results

Table 4.3: Initial quantification of the GaAs wafer done in AZtec. The quantification is done with both SEM and TEM methods. (Brynjar: The idea was to use both AZtec and HyperSpy, but it did not make sense to use HyperSpy with the discussion I have now. Thus it is only AZtec.)

V_{acc}	SEM		TEM	
	Ga	As	Ga	As
5 kV	50 %	50 %	50 %	50 %
10 kV	50 %	50 %	50 %	50 %
15 kV	50 %	50 %	50 %	50 %
30 kV	50 %	50 %	50 %	50 %

To do the quantitative analysis, HyperSpy needs k-factors from AZtec. The k-factors for Ga and As are given in Ta-

ble 4.4. These k-factors are from the GaAs bulk wafer, and AZtec have estimated them theoretically. **(Question for Ton: Shall I list the other k-factors for the other sample areas? I do not think I will use them, since I've only quantified the GaAs bulk wafer. But the other k-factors are results too. Eventually including NW data too, but I do not know that ratio.)**

Table 4.4: K-factors for Ga and As, extracted from AZtec. All the k-factors are theoretically estimated. AZtec provides either the k-factor for the $L\alpha$ or the $K\alpha$ line, and selects automatically based on the energy of the incident electrons.

V_{acc} [kV]	Line	Ga k-factor	As k-factor	Ga / As k-factor ratio
5	$L\alpha$	1.21	1.086	0.898
10	$L\alpha$	1.31	1.223	0.934
15	$L\alpha$	1.331	1.259	0.946
30	$K\alpha$	4.191	3.268	0.780

The initial quantification was done on the data from the GaAs wafer in AZtec. The results are presented in Table 4.3. AZtec can treat the data as both TEM and SEM data, and the results were quantified with both methods. The wafer is a 1:1 alloy of gallium and arsenic, so the atomic percent of Ga and As should be 50% and 50% respectively.

To better understand the ratios between Ga and As, the areas under the peaks in the spectra were counted. Table 4.5 gives the ratios between the areas under the peaks for 5, 10, 15 and 30 kV. The table compares $L\alpha$ peaks, $K\alpha$ peaks, $K\beta$ peaks and the sum of the peaks. The table also lists the FWHM of the peaks.

One of the adjustments explored was the affect of the calibration on the quantification. Using different the calibrations in Table 4.1 gave different quantification results when using CL in HyperSpy. The results are presented in Table 4.6. The same method was used on all spectra, but the quantification on 10 and 15 kV are obviously wrong.

Chapter 5

Discussion

The discussion is presented in this chapter. Producing code from scratch is both a time-consuming process and a learning process. While developing the code, the author learned a lot about EDS analysis and ideas emerged for how EDS analysis could be improved. This chapter begins with an initial discussion of the qualitative results, and then it connects the sub-problems to the results and work done in the project. The order of the sub-problems is the same as in Chapter 1, which is based on the work process. The chapter ends with a discussion of the Main problem 1.

5.0.1 General results from the spectra

All the spectra have peaks with high peak-to-background ratio. In all the spectra, the highest peak is below 5 keV. The zero peak starts before 0 keV and has its maximum at 0.008 keV. The GaAs, NW and Mo spectra show clearly that the peaks broaden with higher E, since they have peaks at low and middle to high energy. The width of the peaks are quantified with FWHM in the quantitative section below. When doing the qualitative analysis, it became clear that the FIB stub was not made of Fe as expected, but rather of Al with a peak at 1.48 keV. All the 5 kV spectra decrease more or less linearly from 1 to 5 keV. Even though the Cu spectra at 30 kV has the Cu $K\alpha$ peak, the Cu $L\alpha$ peak is completely missing. (Brynjar: Add transition sentence.)

Some peaks in the spectra are overlapping, which shifts the shape of the peaks. An example of this is the As $K\alpha$ peak and the Ga $K\beta$ peak in the NW and the GaAs bulk wafer spectra. These peaks are overlapping, but also far enough apart that the peaks are still distinguishable. Another example of overlapping peaks is the Mo $L\alpha$ peak and the Mo $L\beta_1$, which are overlapping so much that they are hard to distinguish. Since they are harder to distinguish, the peak fitting makes one Gaussian for the two peaks, which is off on both peak centers. Overlapping peaks makes counting the signal from specific peaks harder. (Brynjar: Figure of double peaks?)

The signal from the background is another factor which makes counting more difficult. In general, background in the

acquired spectra is low, but with different shapes. In the GaAs, Si and Mo the height of the background decrease with higher acceleration voltage. The background in the Cu spectra increase with higher acceleration voltage. The most similar background signal over different voltages are in the NW spectra. The values of the background radiation is in general very low and almost flat above the highest peak in the spectra. The Al spectrum background is high before the high Al $K\alpha$ peak, and much lower after the high peak. Both the value and the shape of the background is different before and after the peak. The same behavior is clearly true in the Si spectra. The peak where the background change is the highest peak, Si $K\alpha$. The background values in Si 30 kV are 10 times higher before than after the highest peak. The background shape in Si 30 kV is almost linear from 0.6 to 1.6 keV, drops to 10% height from 1.6 to 1.9 keV, and then follows the expected background shape from 1.9 keV. The expected background shape is illustrated in **(Brynjar: Make a drawing of the background.)** All the other spectra show the same behavior with their highest peak and the peaks effect on the background as the Al and Si spectra. In general, the background signals are low, but their different shapes and heights makes it harder to fit the peaks of the characteristic X-ray lines. **(Brynjar: Figure of background? And figure of fit of background before and after a tall peak?)**

In addition to the characteristic peaks and the background, there are also artifacts and strays in the spectra. All the spectra have signal from the $K\alpha$ line of C and O, which could be contamination and oxide layers. The C and O signal is higher at lower acceleration voltage. All the spectra have a Si peak at 1.74 keV. For all but the Si spectra, the Si $K\alpha$ peak at 1.74 keV is a stray from outside the beam or the Si escape peak from the detector. Some spectra have additional signals from elements outside the area of the main beam, like the Mo, Sb and Cu peak in the NW spectra. The Sb peaks in the NW spectra are at 3.60, 3.85, 4.10 and 4.35 keV, being the $L\alpha_1$, $L\beta_1$, $L\beta_2$ and $L\gamma_1$ peaks. All four Mo spectra have a peak at 0.175 keV, which match best with B $K\alpha$ at 0.183 keV. **(Brynjar: Figure of strays?) (Brynjar: Finishing sentence for the general observations.)**

5.1 Analysis steps in HyperSpy

Sub-problem 1 was to do qualitative analysis of the GaAs wafer in AZtec and HyperSpy. The analysis was done as an out-of-the-box analysis, i.e. just following the steps in the documentation. AZtec has a GUI for analysis, but it is not possible to see what is done with the data at the different steps. HyperSpy have documentation online, and the following subsections explain how the analysis was done in HyperSpy.

Each subsection starts with some code lines, followed by an explanation of what the lines do. All variables inside crocodile need to be set by the user, e.g. `<element_list>` would be set to `['Ga', 'As']` for the GaAs wafer. An example notebook with quantification of the GaAs wafer is attached in APPENDIX. **(Brynjar: Make a notebook with GaAs quantification in HyperSpy, with the data somehow.)**

5.1.1 Loading the data and specifying the elements

```
s = hs.load(<filepath>, signal="EDS_TEM")  
  
s.set_elements(<element_list>)
```

The first step in the analysis is to load the data as a HyperSpy signal type, and specifying the signal as TEM. The signal type is a class in HyperSpy that contains the data and the metadata, and it has methods for analysis. The signal type must be specified as TEM, because the signal type for SEM is very limited and does not have a method for quantification. When using .emsa files from AZtec, as is done in this project, the metadata contains some relevant and some irrelevant information. The information relevant later in this project is: acceleration voltage, dispersion, zero offset, energy resolution Mn $K\alpha$. After loading, it is possible to plot the data with `s.plot()`.

Already at this point there is a big problem with using HyperSpy on the acquired data: the analysis methods are not implemented for SEM but for TEM. As explained by Skomedal in her master's thesis [6], the quantification with the Cliff-Lorimer method of TEM EDS data use approximations which are valid for thin samples. The approximation is that the sample is thin enough to ignore absorption and fluorescence, which is a very crude approximation to use on bulk SEM EDS data. Still, the results show that it is possible to quantify the elements in the GaAs wafer with the Cliff-Lorimer method and get plausible results, but also that the analysis breaks down occasionally. Implementing quantification from the SEM type signal in HyperSpy have been discussed on the repositories GitHub issues page¹. The topic have been discussed in 2020, 2017 and 2015. People have been working on quantification of SEM EDS data, but the work have not been finished yet.

The quantification done with the CL method in HyperSpy on the three different calibrations in Table 4.6 are all within 10% of the expected composition. Carter and Williams [1, p. 612 and 648] state that the accuracy of EDS is at best $\pm 3-5\%$, but that it could be reduced to around $\pm 1.7\%$ with very long acquisition times and a careful analysis. Carter and Williams claim that quantitative errors less than $\pm 5-10\%$ takes a lot of time and effort, and compositions with error below 5% should be regarded extra carefully and with suspicion. The best result, i.e. the result closest to 50%, from the HyperSpy CL quantification is strangely from the AZtec calibration with a 6.25% error. It is strange that the AZtec calibration is the best, because that is the calibration which misses most on the line accuracy in Table 4.2. This implies that the calibration is not the most important factor for the quantification, at least not when the calibration is around $\pm 1\%$. The different calibrations are discussed further in Section 5.3. In the 30 kV GaAs sample the signal-to-noise ratio is good, the sample time was long and the peaks are well resolved, which make the input data good and allows for better quantification. The CL method is known to work on SEM data, but normally one would also do the ZAF correction, which is described in chapter 19.10.3 of Goldstein [2]. The ZAF correction adjust the signal for the atomic number effect, the absorption in the bulk of the sample and the X-ray fluorescence of new lines with lower energy than the initial characteristic X-ray. Since Ga and As are number 31 and 33 in the periodic table, it could be that the ZAF

¹<https://github.com/hyperspy/hyperspy/issues/2332>

corrections are small and would not have a big effect on the results. When doing the quantification it was tested to include O and C, but that changed the results from plausible to completely wrong. The quantification analysis also broke down when using the 10 and 15 kV spectra, but the reason for that was not clear. The breaking down of the analysis is discussed further in [Section 5.5](#).

Results in this project show that the CL method in HyperSpy for TEM EDS data sometimes yield plausible results on SEM EDS data and sometimes break down, thus the method should be used with caution. The goal of this project was not to do or to implement cutting edge quantification of EDS data from a SEM sample, but rather to understand the analysis steps and what factors that could affect the results. Thus, using the quantification method from the TEM signal type was regarded as good enough for this project.

5.1.2 Removing the background linearly

```
bw = s1.estimate_background_windows(windows_width=<number>)
```

```
iw = s1.estimate_integration_windows(windows_width=<number>)
```

The next step is to remove the background, which with the above code is done by a linear fit. The background can be removed through model fitting, which is covered in [Section 5.1.4](#). The variable `windows_width` sets how wide the windows are for the background and integration, measured in FWHMs. A good starting value for `windows_width` is 2, but it should be tested by the user with a plot to see if the background will be removed correctly. The estimated windows can be plotted with:

```
s.plot(xray_lines=True, background_windows=bw, integration_windows=iw)
```

Plotting has proven to be a very useful tool for understanding what the different steps in the analysis do. Unfortunately, the implemented plotting in HyperSpy is limited. For example, when plotting a modelled spectrum with Ga and As, the model contains all the peaks in the HyperSpy library and all the peaks are plotted, but it is not possible to see what the different peaks are. In other words, the plot of a model can show all the independent components, but adding a legend is not an option. Another limitation of the plotting is the interactivity when saving the plot. Matplotlib requires the code to run in the background for it to be interactive, while Plotly can save the plot as an interactive HTML file for later inspection. One of the advantages with the plotting in HyperSpy is how accesable it is to plot in the different steps, which the user can use to understand and verify the analysis. The HyperSpy plotting was probably not made with the intention of being used for publication, but rather for quick and easy plotting of the data. If that is the case, the plotting serves its purpose well and has proven to be very useful for this project.

One of the more helpful insights from plotting in this project was that removing the background is not trivial. This is especially true for background signals modelled as a polynomial. Linear background removal works well for some peaks, for example the K-lines of Ga and As, but not for the L-lines. The background around the K-lines are more

linear, because of the exponential decay of the background. Around the L-lines the background is affected by the absorption of the Bremsstrahlung lower than 2 keV and the observation of higher background levels below the highest peak in the spectrum. The background removal is discussed further in Section 5.4.

5.1.3 Quantification after linear background removal

```
s_i = s.get_lines_intensity(background_windows=bw, integration_windows=iw)

k_factors = [<k-factor 1>, <k-factor 2>]

quant = s.quantification(s_i, method='CL', factors=k_factors)

print(f'E1: {quant[0].data[0]:.2f} \%, E1: {quant[1].data[0]:.2f} \%')
```

The quantification is done with the four lines of code above, where the last one prints the results. The first line gets the intensity of the peak corresponding to the lines of the specified element. HyperSpy selects automatically which lines to use for quantification. To see which lines are used, the `s_i` variable can be printed. The second line sets the k-factors. The k-factors in this project have been the one from AZtec, which are theoretically estimated. The third line does the quantification, where the method is specified. The method is the Cliff-Lorimer method, described in detail in Mari Skomedal's master thesis [6, Sec. 2.2.3]. HyperSpy has a method for quantification with the zeta factor method. The zeta method requires the value for the beam current, which was not measured in this project. ²

The k-factors are essential for the Cliff-Lorimer quantification, and the k-factors listed in Table 4.4 give some insight into how AZtec calculates the k-factors. From the results it is clear that AZtec at least adjust the k-factor for element and for voltage. It could be that factors like the beam current and time live could affect the k-factor, but this was not investigated in this project. The L-line k-factors are start at 1.1 for 5 kV and increase to 1.2 for 15 kV. The As k-factor for the L-line at 5, 10 and 15 kV is 11%, 7% and 6% greater than for Ga. The K-line k-factor are 3.3 for Ga and 4.2 for As, implying either a high sensitivity for higher voltages or two different models for calculating the k-factors. Another possibility is that the K-lines and L-lines have a separate model for calculating the k-factors. This can be tested by extracting the k-factors for the K-lines from the 15 kV spectrum, as the 15 kV spectrum do have peaks for both the K-lines and L-lines. The k-factors for Ga are in all four cases higher than for As, which makes sense, as all the Ga lines are higher and have more counts than the As lines. Quantification of the ratio between the Ga and As peaks are done in Table 4.5, where it is clear that the k-factor push the ratio towards 1. The peak ratio times the k-factor for 5 kV is 1.1, and the next closest to 1 is 1.3 for 30 kV. This result imply that the theoretically calculated k-factors could be better for high and low voltages.

(Question for Ton: I am happy with the discussion until this point (08.12.22). How would you rate it?)

²Results from the zeta method can be converted to the cross section method, see the page "EDS Quantification" in the HyperSpy documentation.

5.1.4 Removing the background with model fitting

Another way to remove the background is to fit a model to the data. This step would be done right after loading the data. If the raw data contains a zero peak, as is the case for most Oxford instrument EDS detectors, the zero peak needs to be removed before fitting the model. The zero peak is removed by skipping the first n channels, where $n=30$ works well with the data from the GaAs wafer. The model fitting is done with the following code:

```
s = s.isig[<zero_peak>:]

m = s.create_model(auto_background=False)

m.add_polynomial_background(order=12)

m.add_family_lines(<list_of_element_lines>)

m.plot()
```

The lines above removes the zero peak, create a model from the signal `s`, adds a 12th order polynomial, add the lines of the elements in the signal, and plot the model. This model is not fitted, it is just a generated spectrum with the lines of the elements. Eventually, the method `create_model()` can take the boolean argument `auto_add_lines=True`, which will automatically detect the elements in the sample. The model consists of a number of components, which can be accessed with `m.components`. The components are all the Gaussian peaks in the spectrum, in addition to the background as a 12th order polynomial. The order of the polynomial can be changed, but it should be tested by the user to see if it is a good fit. Further, the model must be fitted.

```
m.fit()

m.plot()
```

The first line fits the model to the data to the components and the second line plots the model. HyperSpy have an own option for fitting only the background. Since the background is one of the components in `m`, it is fitted with the code line above.

5.1.5 Quantification after model fitting

```
m_i = m.get_lines_intensity()

k_factors = [<k-factor 1>, <k-factor 2>]

quant = s.quantification(s_i, method='CL', factors=k_factors)

print(f'E1: {quant[0].data[0]:.2f} \%, E1: {quant[1].data[0]:.2f} \%')
```

The quantification after model fitting is done in the same way as in Section 5.1.3, but with intensity from the model instead of the signal. When modelling GaAs, the model can add the intensity from both K-lines and L-lines. Since

AZtec only gives the k-factors for either the K-lines or the L-lines, the user must remove the lines without k-factors before quantification.

5.1.6 Calibrating the spectrum with the HyperSpy model

```
m.calibrate_energy_axis(calibrate='scale')
```

```
m.calibrate_energy_axis(calibrate='offset')
```

The two lines above calibrates the spectrum with the HyperSpy model and updates the dispersion and zero offset. The metadata in the `signal.s` is updated with the new calibration. Thus, doing the previous step with quantification after model fitting can give a more correct quantification.

5.2 Peak and background modelling

The next sub-problem was to find out how the peaks and the background are modelled in a way that is easy to understand. The model was built without HyperSpy, with the idea of making every step easier to understand. The model was used to be able to remove the background and be able to calibrate the spectrum. The model was compared to the HyperSpy model. The model could be used to quantify the elements in the sample, but this was not done in this project. (Brynjar: Do I want to do this?)

The first step in creating a model is to identify the peaks. The peaks are assumed to be Gaussian curves. The initial way of identifying peaks was that the user manually identified the peaks. Later the peaks were identified with the function `find_peaks()` from the `scipy.signal` package. Different peak prominence were tested, and the peak prominence of 0.01 gave the best results.

The second step is to make a Gaussian in each peak and one polynomial for the background. To do the fitting, the components need an initial guess. The background needs a coefficient for each order of the polynomial. Each Gaussian need to have a mean, a standard deviation, and a height. The mean is the peak position. The standard deviation is the width of the peak, where $FWHM = std * 2 * \sqrt{2 * \ln 2}$ ³. The height is the amplitude of the peak. The easiest way to get the initial guesses for the Gaussians is to normalize the data and set all three parameters to 1. In the normalization the highest peak was set to 1, and the rest of the peaks were scaled accordingly. The best way to get the initial guesses for the background is to clip out the peaks with linear interpolation and fit a polynomial. The initial guesses for the background are then the coefficients of the polynomial. With the initial guesses, the whole model is ready to be fitted.

The third step is to fit the model to the data. Using the `curve_fit()` function from the `scipy.optimize` package, the model is fitted to the data. The function `curve_fit()` uses the Levenberg–Marquardt algorithm to fit the model to the data. The function `curve_fit()` returns the optimal parameters for the model. Fitting both the Gaussians

³FWHM defined at: https://en.wikipedia.org/wiki/Full_width_at_half_maximum

and the background at the same time makes the fitting more stable. One of the first iterations, where the user manually inputted the peaks, the fitting tended to partially fail. The issue was that the fitting only was done on the peaks. To minimize the error in the fitting, one of the Gaussian curves with a low amplitude was moved and got a huge standard deviation, which compensated the background. This was fixed by fitting both the Gaussians and the background at the same time. Doing this made the fitting both better, and it failed less often.

(Brynjar: Issue: fitting e.g. Mo with two clear peaks, but not with enough prominence to be found by the peak finder.)

5.3 Calibration

The next sub-problem was to calibrate the data with a self produced Python script. With a fitted model of the spectrum, the calibration can be done. Calibration can both be done on raw data with channels on the x-axis and on poorly calibrated data with energy on the x-axis. The dispersion is calculated with Equation (2.10). Table Table 4.1 shows calibration from AZtec, HyperSpy, and the self produced Python script.

5.4 Background models

The next sub-problem was to find out how different background models affect the quantitative analysis done in HyperSpy, and how well different order polynomials fit the background. The background models were tested on the spectrum of GaAs, and later also on **(Brynjar: TODO: other spectra. Also make a table here with results)**. The background was modelled as a polynomial of different orders. To quantify the different background models, the residuals were calculated. The residuals are the difference between the data and the model. **(Brynjar: Use root-mean-square error?)** The TABLE XXXX **(Brynjar: make table)** shows the residuals for the different order background models. The best orders were visually inspected. A later idea was to model the background as a spline, which is a piece wise polynomial. The spline is a piece wise polynomial with a smooth transition between the pieces. The spline was not tested in this project, but it could be a good alternative to the polynomial background model.

5.5 Analysis failure

The next sub-problem was to find out when the analysis fails, both in AZtec and HyperSpy.

(Question for Ton: Section about normalization too?)

5.6 Calibration decision

5.7 Choices in HyperSpy

Bibliography

- [1] C.B. Carter and D.B. Williams. *Transmission Electron Microscopy: Diffraction, Imaging, and Spectrometry*. Springer International Publishing, 2016.
- [2] Joseph I. Goldstein, Dale E. Newbury, Joseph R. Michael, Nicholas W.M. Ritchie, John Henry J. Scott, and David C. Joy. *Scanning Electron Microscopy and X-Ray Microanalysis*. Springer New York, New York, NY, 2018.
- [3] J. Michael Hollas. *Modern spectroscopy*. J. Wiley, Chichester ; Hoboken, NJ, 4th ed edition, 2004.
- [4] Daniel Lundeby. Improving the accuracy of TEM-EDX quantification by implementing the zeta-factor method. Master's thesis, Norwegian University of Science and Technology, 2019.
- [5] Manne Siegbahn. Relations between the K and L Series of the High-Frequency Spectra. *Nature*, 96(2416):676–676, February 1916.
- [6] Mari Sofie Skomedal. Improving quantitative EDS of III-V heterostructure semiconductors in low voltage STEM. Master's thesis, Norwegian University of Science and Technology, 2022.
- [7] Albert C Thompson, David T Attwood, Malcolm R Howells, Jeffrey B Kortright, Arthur L Robinson, James H Underwood, Kwang-Je Kim, Janos Kirz, Ingolf Lindau, Piero Pianetta, Herman Winick, Gwyn P Williams, and James H Scofield. *X-Ray Data Booklet*. Lawrence Berkeley National Laboratory, University of California, 2nd ed edition, 2004.